Journal of Applied Physics

Suitability of metallic materials for constructing metal-coated dielectric terahertz waveguides

Cite as: J. Appl. Phys. **131**, 105106 (2022); https://doi.org/10.1063/5.0075639
Submitted: 17 October 2021 • Accepted: 13 February 2022 • Published Online: 11 March 2022

Yuyuan Huang, Kuniaki Konishi, Momoko Deura, et al.

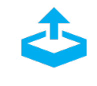

ARTICLES YOU MAY BE INTERESTED IN

Simplified Timoshenko-Ehrenfest beam equation to analyze metamaterials
Journal of Applied Physics **131**, 104902 (2022); https://doi.org/10.1063/5.0077001

Soliton-like surface waves propagating along the interface between a metamaterial and an antiferromagnet
Journal of Applied Physics **131**, 105302 (2022); https://doi.org/10.1063/5.0079233

Achieving superconductivity with higher T_C in lightweight Al–Ti–Mg alloys: Prediction using machine learning and synthesis via high-pressure torsion process
Journal of Applied Physics **131**, 105903 (2022); https://doi.org/10.1063/5.0086694

Lock-in Amplifiers up to 600 MHz

© 2022 Author(s).

Journal of Applied Physics ARTICLE scitation.org/journal/jap

Suitability of metallic materials for constructing metal-coated dielectric terahertz waveguides

Cite as: J. Appl. Phys. **131**, 105106 (2022); doi: 10.1063/5.0075639
Submitted: 17 October 2021 · Accepted: 13 February 2022 ·
Published Online: 11 March 2022

View Online

Export Citation

CrossMark

Yuyuan Huang,[1] Kuniaki Konishi,[2] Momoko Deura,[1] Yusuke Shimoyama,[1] Junji Yumoto,[2,3] Makoto Kuwata-Gonokami,[2,3] Yukihiro Shimogaki,[1] and Takeshi Momose[1,a)]

AFFILIATIONS

[1]Department of Materials Engineering, The University of Tokyo, 7-3-1 Hongo, Bunkyo-ku, Tokyo 113-8656, Japan
[2]Institute for Photon Science and Technology, The University of Tokyo, 7-3-1 Hongo, Bunkyo-ku, Tokyo 113-0033, Japan
[3]Department of Physics, The University of Tokyo, 7-3-1 Hongo, Bunkyo-ku, Tokyo 113-0033, Japan

[a)]**Author to whom correspondence should be addressed:** momo@dpe.mm.t.u-tokyo.ac.jp

ABSTRACT

We aimed to identify metallic materials that could be used to construct metal-coated dielectric terahertz (THz) waveguides. We examined seven different metals: gold (Au), copper (Cu), silver (Ag), aluminum (Al), nickel (Ni), chromium (Cr), and titanium (Ti). The propagation losses of our in-house metal-coated dielectric parallel-plate waveguide (PPWG) were experimentally determined. We developed a physical model to estimate the two key parameters determining the performance of metal-coated waveguides: the critical film thickness required for bulk material-like behavior and the propagation loss in a film with a thickness greater than critical film thickness. Film quality, as revealed by the thickness-dependent electrical conductivity of the metal film, was measured prior to experiments and used for model calculations because propagation loss is influenced by film conductivity, which differs from bulk conductivity and depends on film thickness. After experimentally validating the applicability of the model to different metals, suitable metals were identified based on the two key parameters calculated by the model, assuming the same high film quality. Cu was identified as the optimal metal. The effect of film quality on the two key parameters is discussed in this paper. The impact of the surface oxide (CuO_x) layer on THz wave propagation was experimentally evaluated using CuO_x/Cu-coated PPWG; no detectable transmittance decrease was observed regardless of the CuO_x thickness (1.5–176 nm), when the underlying Cu film was of sufficient thickness. Our model also indicated that a CuO_x layer <1 μm-thick had a negligible impact on THz wave propagation. Thus, native oxidation is not an issue when using Cu.

Published under an exclusive license by AIP Publishing. https://doi.org/10.1063/5.0075639

I. INTRODUCTION

Terahertz (THz) wave technology is an emerging field with applications in communication, agriculture, security, medicine, and Earth sciences.[1–5] The application of THz wave-based communications is anticipated in beyond-fifth-generation and sixth-generation networks;[6] it has led to the development of THz passive devices, including filters, resonators, antennas, and waveguides.[7–10] Waveguides are essential communication system components that guide and propagate waves, but they are challenging to fabricate because their aperture sizes are on or below the submillimeter order.[11] Thus far, THz waveguides have typically been composed of two discrete pieces (i.e., split-block configuration).[12–14] This structure inevitably experiences substantial misalignment loss when the two split blocks are assembled into a single component, thus degrading waveguide performance; such loss becomes significant with increasing frequency, especially when the split blocks are connected with other passive components.[15] Therefore, monolithic devices must be developed to fully utilize the intrinsic performance of THz wave devices and integrated devices. Three-dimensional printing has been regarded as a potential solution for this problem because it can construct complex monolithic structures with sufficient resolution.[16–18] Notably, high-resolution three-dimensional printing can only manage dielectric materials, such as polymers; therefore, metal films are necessary to coat the polymer substrate to prevent THz wave penetration loss. However, the thin-film technology necessary for creating metal-coated dielectric devices by depositing a metal film onto the entire three-dimensional surface of a submillimeter-scale, high aspect ratio, hollow structure has not yet been developed. Thus, the development of thin-film technologies that can achieve conformal deposition is essential for realizing

Published under an exclusive license by AIP Publishing

monolithic metal-coated dielectric THz waveguides and further integration candidates (e.g., chemical vapor deposition, atomic layer deposition, and supercritical fluid deposition).[19–23]

Two additional questions must be answered for the development of metal-coated dielectric THz wave devices: what is the optimal film thickness, and what material should be employed? The answers to both questions depend on the material properties, which must, therefore, be studied. A few pioneering works on the THz properties of metal films (as revealed by plasmon waves) have been published.[24,25] The film must be sufficiently thick to allow it to behave as a bulk material,[26] but excessive thickness increases material costs and reduces throughput; furthermore, film thickness is influenced by film quality. We previously investigated the critical thicknesses of gold (Au) films and their propagation losses using our in-house multi-channel Au-coated silicon (Si) parallel-plate waveguides (PPWGs) as test structures. We then developed a physical model to explain and anticipate thickness-dependent propagation loss and the critical film thickness.[27] Note that critical film thickness was previously defined as the thickness associated with a loss 10% greater than that of 500-nm-thick films; we use this definition in the present work. Our model showed that the overall propagation loss involved penetration and ohmic loss components; we calculated their relative contributions. Penetration loss occurs when a THz wave passes through a very thin metal film into the dielectric substrate; thus, such loss depends on film thickness. Ohmic loss occurs when an electric current dissipates in the film and thus depends on electrical conductivity (determined mainly by impurities and grain boundaries). For very thin films (typically below several hundred nanometers in thickness), film conductivity also depends on film thickness, decreasing with reduced thickness because of increased electron scattering on the surface/interface of the metal film (i.e., the thin-film effect) (Fig. S1 in the supplementary material). Our model also showed that the critical film thickness is determined by the penetration loss in the GHz region, but by the ohmic loss (i.e., electrical conductivity) in the THz region. In detail, the critical film thickness in the GHz region is the minimum thickness (typically >500 nm) that prevents penetration loss; this thickness decreases with increasing frequency in the GHz region as the skin depth decreases. In the THz region, the thickness required to prevent penetration loss is very small (typically <100 nm), but the use of such a thin film causes significant ohmic loss attributable to the lower conductivity associated with the thin-film effect. Therefore, the critical film thickness in the THz region is the minimum thickness associated with a drop in conductivity caused by the thin-film effect. For our fabricated Au films, the critical film thickness decreased with increasing frequency in the GHz region (0.03–1.0 THz) but increased in the THz region (1.0–3.0 THz); the representative thicknesses were 453, 171, and 225 nm at 0.03, 1.0, and 3.0 THz, respectively.

Au has typically been used to prepare metal-coated dielectric THz wave devices because of its high conductivity and high oxidation resistance.[28–30] However, because of high material cost, the practical applications of Au coating for THz wave devices are limited. Thus far, suitable alternative metals have not been identified because there is a lack of quantitative and systematic evaluation based on material science and engineering, although silver (Ag) and copper (Cu) have been considered for practical application.[31,32] The use of ferromagnetic materials such as nickel (Ni) has also been proposed.[33] In addition, given that the dominant factor of propagation loss changes from penetration to ohmic when the frequency transitions from the GHz to THz region (as explained above), materials that are suitable in the GHz region are not necessarily appropriate in the THz region. Thus, material evaluations should consider the effect of ohmic loss. Evaluation must be systematic; the propagation losses of different materials must be examined under identical conditions. Thickness dependence must also be considered. The use of an arbitrarily fixed thickness is inappropriate because the propagation loss in the THz region (ohmic loss-dominant) depends on film thickness (the thin-film effect may be in effect).[27] Thus, our method evaluates the two key parameters that affect waveguide performance: the critical film thickness and propagation loss in a film with a thickness exceeding that value.[27] As all metals except Au form native oxide layers on film surfaces, the impact of these oxides on THz wave propagation must also be examined. Although oxides are conventionally thought to be harmful, no systematic study has yet been performed.

Appropriate film formation processes are required. We found that critical film thickness and propagation loss were influenced by electrical conductivity. Thus, a high-quality (i.e., high electrical conductivity) film is essential for simultaneous enhancement of waveguide performance and suppression of critical film thickness. Chemical vapor deposition, atomic layer deposition, and supercritical fluid deposition methods ensure high conformality[34–36] and yield high-purity films. These techniques are associated with much smaller critical film thicknesses than those of current electroplating technologies; this compensates for the lower deposition rates of the former methods.

In this study, we screened suitable metallic materials for the construction of metal-coated dielectric THz wave devices based on the two key parameters calculated by the model, assuming the same high film quality.[27] Prior to screening, we experimentally validated our model for various metals. We used our in-house PPWGs; silicon served as the dielectric substrate to ensure a flat surface morphology and uniform film thickness of the metal coating. We used sputtering to yield high-quality films with smooth surface morphology and precise thickness. We employed THz-time domain spectroscopy (THz-TDS) to measure the propagation losses of metal-coated PPWGs.[37] The reason we chose THz-TDS is for rapid measurements for our comprehensive study that necessitates a large number of measurements with various metals and film thicknesses. Note that these test structures were used only for material selection; they were not employed in applications. The physical model is explained in Sec. II and the experimental details are provided in Sec. III; after the experimental validation of model, the critical film thickness and propagation loss in a film with greater than critical film thickness are evaluated for seven metals [Au, Cu, silver (Ag), aluminum (Al), Ni, chromium (Cr), and titanium (Ti)] in Sec. IV. The impact of the surface oxide (CuO_x) layer on THz wave propagation was evaluated in Sec. V. An appropriate deposition method for the fabrication of metal-coated dielectric THz waveguides is discussed in Sec. VI. Finally, we investigate the generality of the PPWG critical film thickness parameter for waveguides of various shapes in Sec. VII.

Published under an exclusive license by AIP Publishing

II. MODEL OF PROPAGATION LOSS FOR A METAL-COATED THZ PPWG

A. Basic model for metal-coated dielectric waveguides

We applied a previously developed model to estimate the propagation loss for a metal-coated dielectric PPWG.[27] The bouncing wave description of the metal-coated dielectric PPWG applied in the model is shown in Fig. 1(a). The model was developed by modifying the bouncing wave of metallic PPWGs.[38] The THz wave is reflected on the surfaces of two parallel plates with a gap distance δ and then propagates at an incidence angle θ in the z-direction. Propagation loss (α) occurs in the metal-coated dielectric PPWG because of imperfect reflection at air/metal and metal/dielectric interfaces. The propagation loss (α_{123}) for a metal-coated dielectric PPWG in the TE_1 mode is expressed as follows:

$$\alpha_{123} = N\left(1 - |r_{123}|^2\right), \tag{1}$$

where N is the number of bounces per unit length (thus, $\cot\theta/\delta$) and r_{123} is the total reflection coefficient in an air/metal/dielectric PPWG; r_{123} can be expressed in greater detail as

$$r_{123} = \frac{r_{12} + r_{23}e^{2kd_2 i}}{1 + r_{23}r_{12}e^{2kd_2 i}}, \tag{2}$$

where r_{12} and r_{23} are the reflection coefficients at air/metal and metal/dielectric interfaces, respectively; d_2 is the thickness of the metal film; and k is defined as $2\pi(n_2\cos\theta_2)/\lambda_0$, where n_2 is the refractive index of the metal film, θ_2 is the incident angle of the THz wave to the metal film, and λ_0 is the free-space wavelength of the THz wave. Because all parameters in Eq. (2) except n_2 and d_2 can be determined by the geometry of the PPWG and the optical properties of the air (n_1) and a dielectric substrate (n_3), α is influenced only by n_2 and d_2, both of which are related to the metal film. Furthermore, n_2 can be expressed by the direct-current conductivity (σ_0) of the metal film under the assumption of the Hagen–Rubens regime[39,40] as follows:

$$n_2 = \left\{\frac{1}{2}\left[1 + \left(\frac{4\pi\sigma_0}{\omega}\right)^2\right]^{\frac{1}{2}} + \frac{1}{2}\right\}^{\frac{1}{2}} + i\left\{\frac{1}{2}\left[1 + \left(\frac{4\pi\sigma_0}{\omega}\right)^2\right]^{\frac{1}{2}} - \frac{1}{2}\right\}^{\frac{1}{2}}, \tag{3}$$

where ω is the angular frequency. In addition, σ_0 significantly decreases with decreasing thickness (i.e., the thin-film effect), which is apparent at <200 nm for Cu (e.g., because of electron grain boundary and surface scattering); therefore, the dependence of film thickness on electrical conductivity should also be considered. Hence, the thickness-dependent electrical conductivity of the metal film $\sigma_{0,f}$ is used instead of σ_0; $\sigma_{0,f}$ is determined by the Fuchs–Sondheimer (F–S) theory and the Mayadas–Shatzkes (M–S) theory[41,42] as a function of d_2 as follows:

$$\frac{1}{\sigma_{0,f}} = \left(\frac{3\times\lambda\times\frac{1}{\sigma_{0,b}}}{8}\times(1-p) + \frac{3\times\lambda\times\frac{1}{\sigma_{0,b}}}{2}\times\frac{R}{1-R}\right)\times\frac{1}{\mathrm{d}_2} + \frac{1}{\sigma_{0,b}}, \tag{4}$$

where $\sigma_{0,b}$ is the bulk conductivity of the metal film, λ is the mean free path of an electron in the metal film, p is the specularity coefficient of the metal film, and R is the grain boundary reflection coefficient of the metal film. Accordingly, it is possible to estimate α_{123} using Eqs. (1)–(4) of our model, considering $\sigma_{0,f}$ (and resulting n_2) and d_2, both of which can be obtained experimentally, and using ω for measurement. Note that a full-vector analysis can theoretically calculate the precise behaviors of millimeter-scale THz electromagnetic waves within metallic films but, given their dimensions, the computational costs are very high. Our model (based on the bouncing wave) is simpler and more concise and feasible, but it still adequately reveals material properties. Note that the model described by Eqs. (1)–(4) deals with THz wave propagation inside the PPWG; however, this can also be applied to our multi-channel PPWG because, although experimental transmittance is influenced by the geometry and materials outside the channel, the propagation loss is not (because it is canceled out during the transition from transmittance to propagation loss).

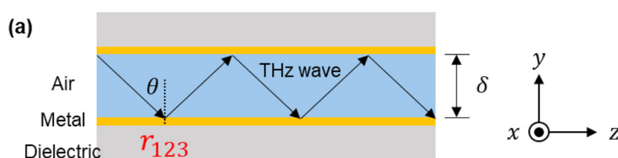

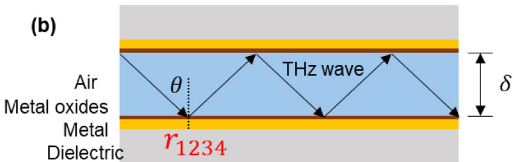

FIG. 1. Bouncing wave description of terahertz (THz) wave propagation in (a) metal-coated dielectric parallel-plate waveguides (PPWGs) and (b) metal oxides/metal/dielectric PPWGs.

B. Extended model for metal-coated dielectric waveguides with surface oxides

To calculate the propagation loss (α_{1234}) of a metal-coated dielectric PPWG including surface oxides on the metal film, reflection at the metal/metal–oxide interface should be further considered. Four mediums must be considered for the PPWG, including air, metal–oxide, metal, and dielectrics [Fig. 1(b)], with refractive indexes of n_1, n_2, n_3, and n_4, respectively. Using Eq. (1), α_{1234} is obtained from the total reflection coefficients of the four-layer

Published under an exclusive license by AIP Publishing

structure (r_{1234}), which is determined as follows:

$$r_{1234} = \frac{r_{12} + r_{23}e^{2k_2d_2i} + r_{34}e^{2(k_2d_2+k_3d_3)i} + r_{12}r_{23}r_{34}e^{2k_2d_2i}}{1 + r_{12}r_{23}e^{2k_2d_2i} + r_{23}r_{34}e^{2k_3d_3i} + r_{12}r_{34}e^{2(k_2d_2+k_3d_3)i}} \left(k_x = \frac{2\pi}{\lambda_0} n_x \cos\theta_x\right), \quad (5)$$

where r_{12}, r_{23}, and r_{34} are the reflection coefficients at the interfaces of air/metal–oxide, metal–oxide/metal, and metal/dielectric, respectively; d_2 and d_3 are the thicknesses of the metal–oxide and metal, respectively. Similar to α_{123}, α_{1234} can be estimated using the thickness and thickness-dependent conductivity of the metal (d_3 and $\sigma_{0,f3}$), as well as the thickness and refractive index of the metal–oxide layer (d_2 and n_2). Unlike metals, the relationship between n_2 and $\sigma_{0,f2}$ for non-conductive materials is unknown; therefore, n_2 is used instead of $\sigma_{0,f2}$, and it can be obtained from previous studies or estimated experimentally. Accordingly, it is possible to estimate α_{1234} using the extended model determined by Eqs. (1) and (3)–(5), considering n_2, $\sigma_{0,f3}$ (and resulting n_3), d_2, and d_3, all of which can be obtained experimentally or from previous studies. Note that the model in Fig. 1 does not consider the thickness of the dielectric substrate, i.e., being assumed as infinite.

III. EXPERIMENT

Two experiments were conducted to screen for suitable metals and to evaluate the impact of CuO_x film on propagation loss. Both experiments utilized the multi-channel PPWG developed in our previous work[27] as both the test structure and platform for systematic analysis. Both experiments involved four similar steps [Fig. 2(a)]. The first step was film preparation, which included metal film deposition on both sides of multiple substrates, followed by oxidation of the surface or deposition of the oxide film if necessary. The second step was the evaluation of film thickness and electrical conductivity. The third step was the stacking of multiple substrates to form the PPWG. The final step was the measurement of PPWG transmittance.

A. Experiments for material selection

The p-doped (1–100 Ω cm) double-side-polished Si wafer (thickness: 280 ± 10 μm) with a size of 14 × 2.5 or 14 × 5.0 mm^2 was used as a substrate without pretreatment. The refractive index n_3 was taken to be $3.56 + 0.21i$; this is the average value of a low-resistivity silicon substrate at 0.2–2.0 THz.[43] Metal films composed of Cu, Cr, Ti, or Ni were deposited on both sides by magnetron sputtering (VTR-150M/SRF; Ulvac, Inc., Kanagawa, Japan) using a power supply of 50 W under an argon pressure of 0.8 Pa, similarly with Au.[27] The thickness of the metal film was then measured by scanning electron microscopy (SEM; JSM-7900F; JEOL, Ltd., Tokyo, Japan). The thickness ranges were 20–450 nm for Au,[27] 30–425 nm for Cu, 223–709 nm for Cr, 144–218 nm for Ni, and 290–929 nm for Ti. The electrical conductivity of the film was measured using a four-point probe (U3402A; Agilent Technology, Santa Clara, CA, USA). As the substrate dimensions were 14 × 5.0 mm^2, and the probe intervals were 1.0 mm, a resistivity correction factor (RCF) of 3.5750 was applied.[44] Ten Au-coated Si substrates were stacked at intervals of 280 μm by sandwiching a pristine Si chip (2.1 × 2.5 or 2.1 × 5.0 mm^2) as a spacer, resulting in a nine-channel PPWG. The PPWG fixed within its plastic holder is shown in Fig. 2(b1). After stacking, the channel sizes at the entrance and exit were evaluated by optical microscopy (ECLIPSE LV100; Nikon Corp., Tokyo, Japan); they had a mean height of 0.28 ± 0.01 mm and mean width of 9.8 ± 0.01 mm. The channel width to height ratio at the entrance plane was 35; therefore, it was approximated as a PPWG rather than a rectangular waveguide (RWG). The transmittances of metal-coated PPWGs with lengths of 2.5 and 5.0 mm were measured in dry air by THz-TDS in TE_1 mode, with a frequency range of 0.4–1.4 THz. The cutoff frequency of the lowest-ordered TE mode (TE_1 mode) was 0.54 THz. Considering that the cutoff frequency of the next possible even-symmetric higher-order mode (TE_3 mode) is 1.61 THz, it was apparent that only the TE_1 mode occurred in our measured frequency range of 0.4–1.1 THz.[38,45,46] A collimated THz beam approximately 3.5 mm in diameter was irradiated to the center of the multi-channel PPWG [Fig. 2(b2)]. We used a nine-channel PPWG to ensure that beam intensity could be measured. We did not use a focused beam, which frequently causes run-to-run errors due to misalignment; instead, we used a collimated beam to ensure the repeatability of measurements performed for systematic

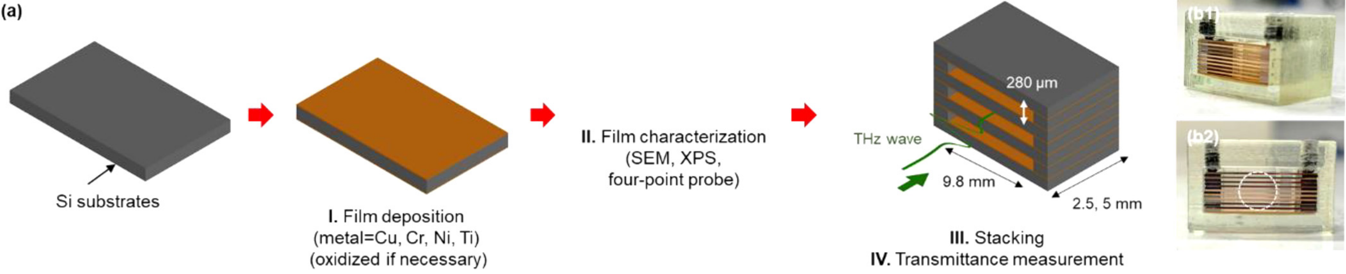

FIG. 2. (a) Fabrication of metal-coated dielectric parallel-plate waveguides. (b1) Side view and (b2) front view of the fabricated sample. The white circle in (b2) shows the position of the irradiated THz beam.

Published under an exclusive license by AIP Publishing

evaluation. Following the measurements, we calculated propagation loss from the transmittances of the 2.5- and 5.0-mm PPWGs as follows:

$$\alpha[\text{dB/m}] = \frac{-10 \times \log \frac{T_2}{T_1}}{L_2 - L_1}, \quad (6)$$

where T_1 and T_2 are the transmittances of waveguides with propagation lengths L_1 and L_2, respectively. Scattering loss caused by the surface roughness of the metal film was not considered because the root mean square value measured by atomic force microscopy (SPA400-DFM; Seiko Instruments Inc., Chiba, Japan) was only 1.0 nm (data not shown). In addition, we simulated transmittance spectra for the same PPWG geometry using perfect electric conductors (PECs); we used commercial software (CST Studio Suite; Simulia, Johnston, RI, USA) for this purpose. A normally incident linearly polarized plane wave that excites the TE_1 mode was directed to the structure when calculating the periodic boundary conditions. As PECs were assumed, the transmittance was not affected by waveguide length.

B. Experiments for impact of CuO_x on propagation loss

To evaluate the impact of CuO_x on propagation loss, we performed an experiment similar to the approach described above, except for CuO_x formation in the second step. The Cu film was deposited to a fixed thickness of 300 nm, which exceeded the critical film thickness (180 nm at 0.72 THz).[27] CuO_x was intentionally formed on the surface of the Cu film using two different methods: by intentionally annealing the Cu film in the air at 80 °C for 1–4 h to form a thin CuO_x film (1.5–7.6 nm) and by depositing a CuO_x film onto the Cu film by magnetron sputtering in an O_2/Ar mixture (0.2 MPa O_2, 0.6 MPa Ar) to form a thick CuO_x film (35–176 nm). The thickness of the thin CuO_x film was characterized by depth profiling of x-ray photoelectron spectroscopy (XPS, model 1600C, ULVAC-PHI XPS, Kanagawa, Japan) coupled with Ar ion etching. The thickness of the thick CuO_x film was characterized by both SEM and XPS; the results showed good agreement. The electrical conductivities of the films were also measured using a four-point probe. These CuO_x/Cu/Si substrates were then stacked as described for the first experiment to form the PPWG. Transmittances of the 2.5- and 5.0-mm metal-coated PPWGs were measured using the methods and conditions described for the first experiment.

IV. MATERIAL SELECTION

To select suitable metal coatings, we evaluated two key parameters that determine the performance of metal-coated dielectric waveguides: critical film thickness and propagation loss in a film thicker than the critical thickness. Note that as an appropriate definition of critical film thickness is lacking, we defined this as the thickness resulting in a loss 10% greater than that of 500-nm-thick films.[27] A 500 nm-thick film was regarded as bulk because it is much larger than the skin depth (e.g., the skin depth is 75 nm for Au at 1.0 THz) and the thickness is such that the electrical conductivity can be regarded as constant; the thin-film effect shown in Fig. S1 in the supplementary material is not in effect, details of which will be explained in Sec. IV C. We experimentally obtained the thickness dependence of propagation loss in metal-coated dielectric PPWGs and compared the results to the values calculated by our physical model based on the thickness-dependent conductivities of metals. The good matching of them verified the validity of our model, so that it was applied for selecting the suitable materials under the assumption that all films were of equal quality. Section IV A presents the transmittance values for the Au, Cu, Ni, Cr, and Ti at various film thicknesses in PPWGs of varying propagation lengths to derive the propagation loss. Section IV B presents the thickness-dependent conductivities of these metals, which are needed to calculate the propagation loss. Section IV C presents the dependence of the propagation loss on the experimentally estimated film thickness based on these results and thereby validates our model. Section IV D presents the materials selected by the model when all films were assumed to be of equal quality.

A. Transmittances of metal-coated PPWGs for various metal films

The transmittances of the Au, Cu, Ni, Cr, and Ti at different film thicknesses for PPWGs of varying length were obtained experimentally to derive the propagation loss. Cross-sectional SEM images used to measure the thicknesses of the metal films are shown in Fig. S2 in the supplementary material. The transmittances are displayed as a function of frequency in Fig. S3 in the supplementary material. Representative results are shown in Fig. 3; the transmittances of 2.5- and 5.0-mm metal-coated PPWGs with 450-nm-thick Au, 425-nm-thick Cu, 218-nm-thick Ni, 709-nm-thick Cr, and 929-nm-thick Ti are shown. The transmittances of PPWGs composed of PEC with the same geometry as the PPWGs used in the study are shown in Fig. 3. Note that multiple oscillations were observed in the simulated transmittances; these indicate multiple reflections at the end face of the waveguide.

For 2.5-mm propagation, the transmittances of Au, Cu, and Ni were as high as the transmittances of PEC-based PPWGs [Fig. 3(a)]. The large difference between the simulated and experimental values near the cutoff frequency is attributable to the fundamental limit of THz-TDS spectral resolution and diffraction loss.[47] In contrast, Cr and Ti exhibited lower transmittances than PEC-based PPWGs, suggesting that the losses were large. Note that Ni exhibited transmittance superior to Cu and Au at certain frequencies [Fig. 3(a)]; this is an artifact (THz-TDS measurement error). In addition, ripples were observed in all experimental, but not simulated, transmittances. These ripples were evident in the THz-TDS transmittances of circular waveguides (CWGs), and in the blank test (i.e., no waveguide),[48] suggesting that the ripples may be THz-TDS-induced artifacts. Although the experimental losses are affected by the errors inherent in transmittance, they were reproduced in the model-calculated losses (Fig. S4 in the supplementary material), suggesting that our experimental transmittances are reasonable. Similar trends were observed for 5-mm-thick PPWG [Fig. 3(b)]. If the films are sufficiently thick, Au, Cu, and Ni showed equally good performance. Because propagation loss is proportional to the square root of permeability,

Published under an exclusive license by AIP Publishing

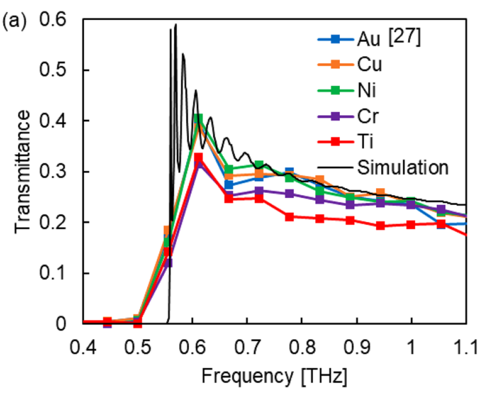

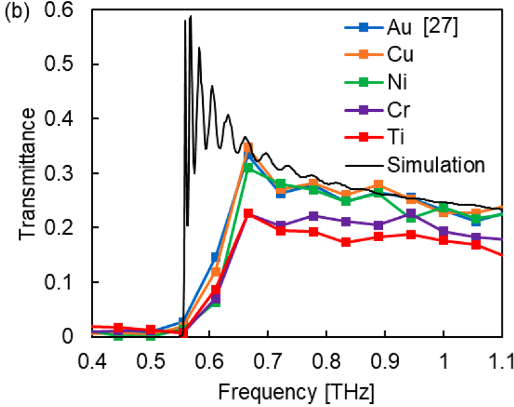

FIG. 3. Transmittances of (a) 2.5-mm- and (b) 5.0-mm-long PPWGs coated with different metals including gold (Au), copper (Cu), nickel (Ni), chromium (Cr), and titanium (Ti), for film thicknesses of 450, 425, 218, 709, and 929 nm, respectively. A model simulation (black line) for a perfect electric conductor (PEC) is added for comparison.

permeability should be considered for ferromagnetic materials such as Ni.[38] However, we observed no detectable decrease in Ni transmittance compared with other non-ferromagnetic materials, which suggests a minor impact of relative permeability in the THz regime. A previous study of Ni permeability in the microwave region[49] showed that permeability decreases to unity when the frequency exceeds 10 GHz, supporting our results. In practice, Ni has been applied in the construction of metal-coated dielectric THz waveguides.[33]

B. Thickness-dependent electrical conductivities of different metals

The thickness-dependent electrical conductivities of the metal films shown in Fig. S2 in the supplementary material are measured. As the reciprocal of conductivity is linearly related to the reciprocal of film thickness [Eq. (4)], the experimental results are plotted in this manner in Fig. 4. Linear regression lines[41] were drawn by fitting the slopes and y-intercepts. The slope represents the strength of the thin-film effect [the terms in parentheses in Eq. (4)] and the y-intercept is the reciprocal of bulk conductivity [last term in Eq. (4)]. The other variables of Eq. (4), including p, R, and λ, are not obtained by fitting. These variables are difficult to estimate theoretically, and thus remain unknown, but it is still possible to discuss thickness-dependent conductivity and propagation loss. As greater conductivity is associated with smaller propagation loss, metal films should have small y-intercepts and slopes. The bulk conductivities (Fig. 4) were 3.7×10^7, 3.7×10^7, 1.1×10^7, 9.1×10^5, and 5.9×10^5 S/m for sputtered Au,[27] Cu, Ni, Cr, and Ti films, respectively. Note that real-world conductivities are always lower than literature values, given the impurities and grain boundaries present in all films. In other words, the literature values were obtained using extremely pure single-crystal metals (e.g., the literature bulk conductivities of Cu and Au are 5.96×10^7 and 4.50×10^7 S/m, respectively).[50] As shown in Fig. 12 in our previous study,[27] the bulk conductivities of Au films prepared using different techniques range from 0.26- to 1.0-fold the literature values. Our Au film had a value close to the literature values, and Cu and Ni values were reasonable. The slopes varied among the metals, suggesting that the magnitude of the thin-film effect depends on the material. Au and Cu performed equally well, showing high bulk conductivity and a small slope, suggesting that both materials would exhibit good propagation performance at any film thickness.

C. Model validation of the various materials

Thickness-dependent propagation loss was estimated from the experimental results reported in Sec. IV A and then used to validate the generality of our model for different metals. Thus, the experimentally obtained transmittances for metal-coated PPWGs with films of varying thickness (depending on frequency; Fig. S3 in the

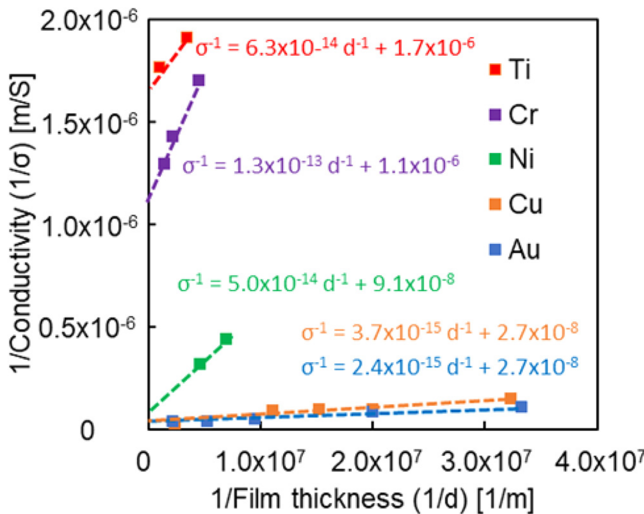

FIG. 4. Relationship between the reciprocals of electrical conductivity ($1/\sigma$) and film thickness ($1/d$).

Published under an exclusive license by AIP Publishing

supplementary material) were converted into propagation losses using Eq. (6). The results are shown in Fig. S4 in the supplementary material. Next, the propagation losses of the Au, Cu, Ni, Cr, and Ti (of varying thicknesses) at 0.72 THz were extracted from Fig. S4 in the supplementary material and are shown in Fig. 5. We chose 0.72 THz because, at this frequency, diffraction loss was not affected by the loss at 0.54–0.70 THz. Therefore, we measured the maximum loss; the loss decreased with frequency, as shown in Fig. S4 in the supplementary material. Frequency-dependent propagation losses were also calculated from the thickness-dependent conductivities of Fig. 4; the results are also shown in Fig. S4 in the supplementary material. Next, propagation loss as a function of film thickness was calculated from the thickness-dependent conductivities (Fig. 4); the results are shown in Fig. 5. The lengths of the error bars in Fig. 5 were determined by measuring the reference (i.e., sample holder alone, without PPWG) five times. For all metals, the experimental and simulated thickness-dependent propagation losses were consistent, thus validating the applicability of our model to different metals. The film thickness-dependencies of the propagation losses at other frequencies (0.78 and 0.84 THz) were also compared (Fig. S5 in the supplementary material); the experiments and simulations were in good agreement. The precise matching at three different frequencies further supports the validity of our model.

The two key parameters of our films that determine the performance of metal-coated dielectric waveguides, i.e., the critical film thickness and propagation loss in a film thicker than the critical thickness, were extracted from Fig. 5 and are shown here for reference. As the critical thickness was defined as the thickness resulting in a loss 10% greater than the bulk, it was necessary to define the bulk. A 500 nm-thick film was regarded as bulk because it is much larger than the skin depth (e.g., the skin depth is 75 nm for Au at 1.0 THz) and the thickness is such that the electrical conductivity can be regarded as constant; the thin-film effect shown in Fig. S1 in the supplementary material is not in effect. Note that as the 500-nm-thick films were not experimentally fabricated, the losses thereof were extracted from the thickness-dependent propagation loss shown in Fig. 5. These were 0.38 dB/cm for Au, 0.41 dB/cm for Cu, 0.87 dB/cm for Ni, 3.5 dB/cm for Cr, and 4.4 dB/cm for Ti. The critical film thicknesses at 0.72 THz were 180 nm for Au, 180 nm for Cu, and 340 nm for Ni, but those for Cr and Ti were not obtained because they exceeded 500 nm. As stated above, our threshold was a loss 10% larger than that exhibited by a 500-nm-thick film. The propagation losses for films exceeding the critical film thickness at 0.72 THz were 0.42 dB/cm for Au, 0.45 dB/cm for Cu, 0.96 dB/cm for Ni, 3.9 dB/cm for Cr, and 4.8 dB/cm for Ti.

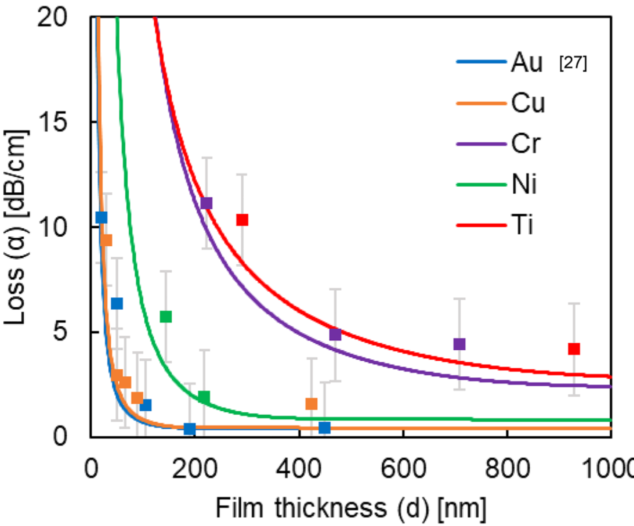

FIG. 5. The thickness dependency of propagation losses at 0.72 THz in PPWGs coated with different metals (Au,[27] Cu, Ni, Cr, and Ti). The dots and lines indicate the measured and simulated values, respectively.

D. Material selection by our model

Given that the validity of our model was confirmed in Sec. IV C, we next used the model to select suitable metals. We recognize that the conductivities ($\sigma_{0,b}$ values) of our deposited films differ from the literature values (e.g., $\sigma_{0,b}$ of our Au film is 0.9-fold the literature value[50] and $\sigma_{0,b}$ of our Cu film 0.6-fold the literature value).[50] It was thus difficult to compare the metals using the deposited films. It is essential to compare different metals while keeping the film qualities consistent, where the qualities are determined by our model from the thickness-dependent conductivity, as given by Eq. (4), which includes $\sigma_{0,b}$ and $[0.375(1-p)(\lambda/\sigma_{0,b}) + 1.5R(1-R)(\lambda/\sigma_{0,b})]$. The latter term denotes the probability of surface and grain boundary scattering, and thus the strength of the thin-film effect; a smaller value indicates higher film quality. During material selection, we made several assumptions about thickness-dependent conductivity. This parameter has been employed for selection of suitable metals that form the interconnections for "ultra-large-scale integration" (ULSI).[51] Thus, p and R were assumed to be the same, and λ and $\sigma_{0,b}$ were taken as the literature values.[52–54] As p and R are not theoretical parameters, and are difficult to determine experimentally, the final value of $[0.375(1-p) + 1.5R(1-R)]$ was assumed to be 0.66. Such a small value indicates a high-quality film; our previous report on the thickness-dependent conductivity of Au films prepared using various deposition methods and experimental conditions[27] showed that the value ranged from 0.66 to 4.8. Under these assumptions, we compared the experimentally studied metals (Au, Cu, Ni, Ti, and Cr), as well as Ag and Al (which also exhibit high electrical conductivity). Note that the metal alloys used for several decades to prepare GHz metallic waveguides[55,56] are also potential candidates; we will evaluate them in the future. In brief, propagation loss according to film thickness was calculated for films of the same quality; we used the thickness-dependent conductivities defined above and Eqs. (1)–(4) (assuming the same p and R, and the ideal λ and $\sigma_{0,b}$). We extracted the key parameters determining the performance of metal-coated dielectric waveguides: the critical film thickness and propagation loss in a film thicker than the critical thickness. It is necessary to determine the bulk for determining the critical thickness, similarly with Sec. IV C, which was also the 500-nm-thick

Published under an exclusive license by AIP Publishing

film herein. The losses in the 500-nm-thick films were obtained from the above calculations as 0.26 dB/cm for Cu, 0.25 dB/cm for Ag, 0.30 dB/cm for Au, 0.34 dB/cm for Al, 0.52 dB/cm for Ni, 0.84 dB/cm for Cr, and 1.5 dB/cm for Ti. Table I summarizes the values used for calculation (i.e., $\sigma_{0,b}$, λ, and $\lambda/\sigma_{0,b}$) and the results (i.e., the critical film thickness and propagation loss of/in films thicker than the critical film thickness [α_{CT}]) for the seven metals. The critical film thickness and α_{CT} values were those at 0.72 THz, i.e., TE_1 mode of our waveguide, as in the experiments. The critical film thickness and α_{CT} values of the different metals listed in Table I are shown in Fig. 6. Note again that these values were obtained under the assumptions described above.[50] The critical film thickness and α_{CT} change with film quality.

A comparison of the two key parameters revealed that Cu was an attractive metal since it had the smallest critical thickness and comparable α_{CT} (with Ag has the smallest value). Considering material cost and availability, Cu should be preferred to Ag and Au. The reasons why Cu exhibited the smallest critical film thickness and comparable α_{CT} (with Ag) are explained below. Critical film thickness is difficult to express using an equation but can be determined from $\sigma_{0,b}$ and $[0.375(1-p)(\lambda/\sigma_{0,b}) + 1.5R(1-R)(\lambda/\sigma_{0,b})]$; the latter term reflects the strength of the thin-film effect. As we assumed that all films had the same p and R values, the latter term was determined by $\lambda/\sigma_{0,b}$ alone. Therefore, the critical film thickness was determined by $\sigma_{0,b}$ and $\lambda/\sigma_{0,b}$. A higher $\sigma_{0,b}$ provides a smaller skin depth and thus a smaller critical thickness. A higher $\lambda/\sigma_{0,b}$ strengthens the thin-film effect; the critical thickness then increases to mitigate the lower conductivity induced by the thin-film effect. Although Ag showed a higher $\sigma_{0,b}$ than Cu, the higher $\lambda/\sigma_{0,b}$ of Ag means that the critical film thickness is greater than that of Cu. α_{CT} is determined only by $\sigma_{0,b}$; a higher $\sigma_{0,b}$ yields a lower α_{CT}. As Cu and Ag have similar $\sigma_{0,b}$ values, the α_{CT} values are also similar. Accordingly, the linear relation between critical film thickness and α_{CT} (Fig. 6) is a consequence of these phenomena.

The impact of film quality on critical thickness is discussed below. The critical thicknesses obtained above are for high-quality films; real-world films are sometimes not of the same quality because of imperfect deposition methods or conditions. Such films generally have higher values of $[0.375(1-p)(\lambda/\sigma_{0,b}) + 1.5R(1-R)(\lambda/\sigma_{0,b})]$ but lower values of $\sigma_{0,b}$, as summarized in our previous study.[27] Figure 7 shows the critical film thickness of a Cu film at 0.72 THz. For the former term, a smaller value indicates a higher-quality film; 0.66 was the lowest literature value that we found.[27] The $\sigma_{0,b}$ of Cu was assumed to vary between 1.4 and 5.96×10^7 S/m; the value of 5.96×10^7 is the literature value.[50] The critical thickness of the highest-quality Cu film was 106 nm (Table I). Lower-quality films exhibiting stronger thin-film effects must be thickened to prevent any such effect, and thereby behave as metallic waveguides {e.g., the thickness is 186 nm for the ideal $\sigma_{0,b}$ with a $[0.375(1-p) + 1.5R(1-R)]$ value of 3.2}. $\sigma_{0,b}$ also influences the critical thickness, which increases as $\sigma_{0,b}$ decreases. For example, when $[0.375(1-p) + 1.5R(1-R)]$ is 3.2, the critical film thickness increases from 186 to 242 nm when $\sigma_{0,b}$ decreases from 5.96×10^7 S/m to one-fourth of that value (1.49×10^7 S/m). Film quality also influences α_{CT} (through $\sigma_{0,b}$ alone); the smaller $\sigma_{0,b}$ values of low-quality films increase α_{CT}. Under such circumstances, it is not necessary to consider the thin-film effect because α_{CT} is the propagation loss above the critical thickness. As α_{CT} is equivalent to the propagation loss of metallic waveguides, it is possible to derive an equation for such waveguides (see below).

Thus, it is clear that both the critical film thickness and α_{CT} are influenced by film quality. Therefore, it is recommended that the thickness-dependent conductivity of metal films be measured prior to fabricating metal-coated THz waveguides. Both key parameters must be addressed. Figure 7 shows how to simply derive the critical thickness from the thickness-dependent conductivity. To minimize the critical thickness and α_{CT}, preparation of high-quality films (via optimization of the deposition method and conditions) is critically important. Although Cu is thought as suitable metals, its critical film thickness and α_{CT} depends on film quality. As the differences in the two key parameters between Ag, Au, Al, and Cu

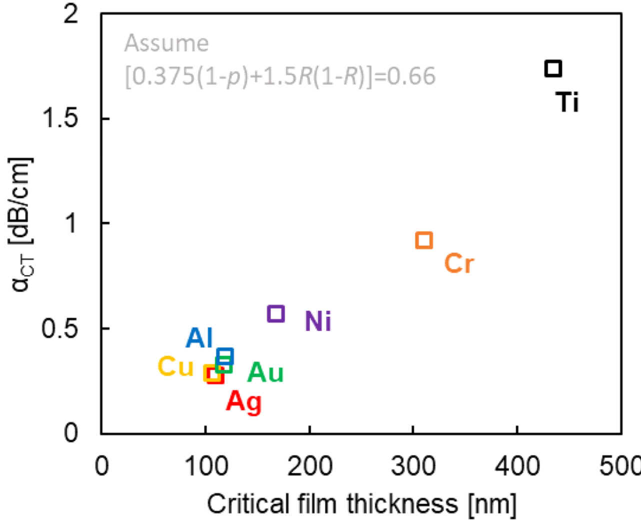

FIG. 6. Critical film thickness and propagation loss in films thicker than the critical thickness (α_{CT}), for various metals. We assumed that $[0.375(1-p) + 1.5R/(1-R)]$ was 0.66. The test frequency was 0.72 THz.

TABLE I. Electrical bulk conductivity ($\sigma_{0,b}$),[50] mean free path (λ),[52–54] quotient ($\lambda/\sigma_{0,b}$), critical film thickness, and propagation loss in a film thicker than the critical film thickness (α_{CT}). We evaluated gold (Au), copper (Cu), nickel (Ni), chromium (Cr), and titanium (Ti) films at 0.72 THz. We assumed that $[0.375(1-p) + 1.5R(1-r)]$ was 0.66 for all metals.

Material	$\sigma_{0,b}$ (S/m)	λ (nm)	$\sigma_{0,b}/\lambda$ (m^2/S)	Critical thickness (nm)	α_{CT} (dB/cm)
Cu	5.96×10^7	39.9	6.69×10^{-16}	106	0.29
Ag	6.30×10^7	53.3	8.46×10^{-16}	110	0.28
Au	4.50×10^7	37.7	8.38×10^{-16}	118	0.33
Al	3.50×10^7	18.9	5.40×10^{-16}	119	0.37
Ni	1.46×10^7	5.87	4.02×10^{-16}	168	0.57
Cr	5.10×10^6	15.2	2.98×10^{-15}	310	0.92
Ti	1.80×10^6	28.5	1.58×10^{-14}	435	1.7

Published under an exclusive license by AIP Publishing

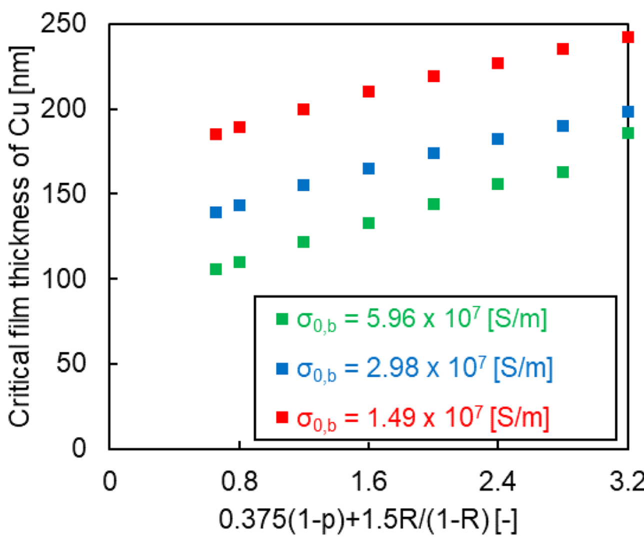

FIG. 7. The critical film thickness of a Cu film at 0.72 THz depending on [0.375 $(1-p)+1.5R/(1-R)$] and the bulk conductivity ($\sigma_{0,b}$). The former value denotes the strength of the thin-film effect on electrical conductivity (a smaller value indicates a higher-quality film; 0.66 was the lowest value that we found).[27] $\sigma_{0,b}$ of Cu was assumed to vary from 1.49 to 5.96 × 10^7 S/m; the literature value is 5.96 × 10^7 S/m.[50]

were small, Ag, Au, or Al could be used if creating such high-quality film are attainable while creating high-quality Cu films are unreachable. Ni, Cr, and Ti should not be used because the values of the two key parameters are not acceptable.

V. IMPACT OF CuO_x ON THZ WAVE PROPAGATION

A. Thin CuO_x layer

We investigated the impact of a thin surface oxide (CuO_x) layer formed on Cu-coated dielectric THz waveguides on transmittance by using a methodology similar to the approach in Sec. IV, except that the metal film surface was intentionally oxidized. Oxidation was conducted by annealing the Si substrate covered by a 300-nm Cu film in air at 80 °C. The thicknesses of the CuO_x layers were 1.5, 3.2, 4.7, and 7.2 nm after 0, 1, 2, and 4 h of annealing, respectively, as evaluated by XPS depth profiling (Fig. S6 in the supplementary material). Cu was consumed by surface oxidation, thereby decreasing the Cu film thickness; however, this reduction was <5 nm in our case, thus providing sufficiently thick Cu under the CuO_x layer. The transmittances of 2.5- and 5.0-mm Cu-coated PPWGs with different CuO_x thicknesses were measured experimentally in TE_1 mode and simulated for PPWGs composed of PEC [Figs. 8(a) and 8(b)]. The transmittances were similar regardless of the CuO_x thickness, PPWG material, and propagation length, within a range of 1.5–7.2 nm. Because the transmittances of the 2.5- and 5.0-mm PPWGs were indistinguishable [Figs. 8(a) and 8(b)], we did not calculate their propagation losses. Because the thicknesses of native CuO_x are reportedly <10 nm at room temperature after several years, such that they remain stable,[57–59] we presumed that the impact of CuO_x on THz wave propagation would be negligible under typical THz wave device operating conditions.

B. Thick CuO_x layer

We also investigated the impact of a thick CuO_x layer on wave propagation because THz wave devices are sometimes used in harsh environments, such as aircraft sensors,[60] where a thick CuO_x layer can form. We used a methodology similar to the approach described in Secs. IV and V A, except that the CuO_x layer was intentionally formed by deposition rather than by annealing. The CuO_x layer was deposited by magnetron sputtering onto an Si substrate covered by a 300-nm Cu film. The CuO_x layer thicknesses were evaluated as described in Sec. V A; XPS depth profiling showed thicknesses of 35, 63, 101, and 176 nm after 15, 30, 60, and 120 s of deposition (Fig. S7 in the supplementary material). These results were consistent with the findings of cross-sectional SEM observation (Fig. S8 in the supplementary material). The

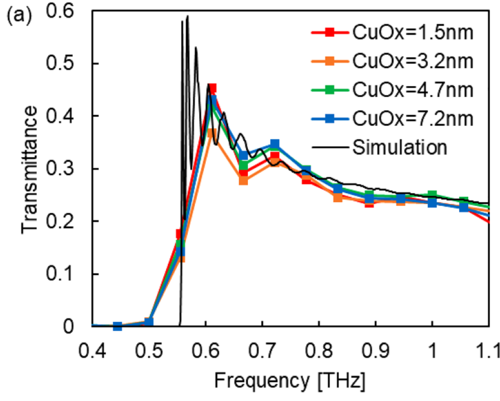

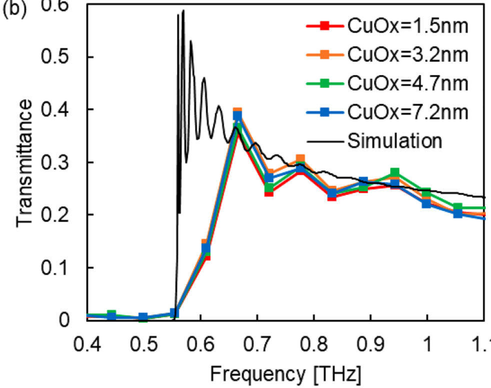

FIG. 8. Transmittance spectra of (a) 2.5-mm- and (b) 5.0-mm-long Cu (300 nm)-coated PPWGs with a thin CuO_x layer on the Cu surface. A corresponding model simulation (black line) for PPWGs composed of PEC is shown for comparison.

Published under an exclusive license by AIP Publishing

transmittances observed for 2.5- and 5.0-mm PPWGs with different CuO_x layer thicknesses and the transmittances simulated for PPWGs composed of PEC are shown in Figs. 9(a) and 9(b). A sample with a 1.5 nm-thick CuO_x layer is shown in Figs. 9(a) and 9(b) for comparison.

Although Fig. 9(a) shows slight between-sample deviations in transmittance at certain frequencies, transmittance did not obviously vary with film thickness. Furthermore, if the CuO_x layer affected transmittance, the magnitude of the effect should be greater at longer propagation lengths [Fig. 9(b)]; in reality, the transmittances overlapped. Therefore, we conclude that there was no difference in transmittance among different CuO_x thicknesses between 2.5- or 5.0-mm PPWGs, or between our in-house PPWGs and PPWGs composed of PEC, indicating that CuO_x did not influence THz wave propagation. Because the transmittances of 2.5- and 5.0-mm PPWGs were indistinguishable [Figs. 9(a) and 9(b)], we did not calculate their propagation losses. Thus, the CuO_x layer had no harmful effects on THz wave propagation, regardless of its thickness.

C. Model-estimated impact of CuO_x layer thickness on propagation losses

The impact of the CuO_x layer on the propagation losses of CuO_x/Cu-coated dielectric PPWGs was investigated theoretically using our extended physical model. The extended model was not experimentally validated because no loss was observed in the experiments, but the results appeared reliable because the extension scheme from metal-coated to metal–oxide/metal-coated waveguide was identical to the extension scheme from a metallic to a metal-coated waveguide. The parameters required for the extended model to calculate propagation losses include the thickness and electrical conductivity of the Cu layer, as well as the thickness and refractive index of the CuO_x layer (see Sec. II B). To focus on the impact of CuO_x layer thickness, we assumed that the underlying Cu film was sufficiently thick (300 nm) to prevent penetration loss, with a conductivity equivalent to the bulk value shown in Fig. 4 (3.7×10^7 S/m). The thickness of the CuO_x layer was varied from 1 nm to 10 μm. The refractive indices for the CuO_x layers were obtained from the literature: $1.9 + 0.04i$ for Cu_2O[61] and $3.1 + 0.06i$ for CuO.[62] These were the values at 1.0 THz but were also applicable in our frequency region (0.7–1.1 THz) because they changed very little with frequency (e.g., the refractive index of CuO ranges from $3.1 + 0.06i$ to $0.07i$ at 0.7–1.1 THz and the refractive index of Cu_2O is $1.9 + 0.04i$ at 1.0–1.1 THz).[61,62]

Because Cu has two oxidation states (CuO and Cu_2O), the impact of the oxidation state on propagation loss was investigated using the extended model. The propagation losses calculated for CuO_x (1 μm)/Cu-coated PPWGs in TE_1 mode with different refractive indices for Cu_2O and CuO are shown in Fig. 10. A Cu-coated PPWG without surface oxide was used as a control. We detected a minor difference between Cu_2O and CuO, i.e., losses of <1.1% and <0.4% (compared to Cu) at any frequency. Such losses may be neglected regardless of the refractive index (i.e., the oxidation state). These results were in good agreement with those for Cu-coated PPWGs without surface oxide, indicating that a 1-μm-thick CuO_x layer is transparent to THz wave propagation, which supports the data shown in Fig. 9. The CuO_x layer did not influence THz wave propagation, regardless of its oxidation state; therefore, the presence of CuO_x is negligible, at least for layers less than 1-μm-thick.

The impact of the thickness of the CuO_x layer on propagation losses was investigated using the extended model. The refractive index of CuO_x was assumed to be constant, independent of its thickness. The propagation losses of CuO_x/Cu-coated PPWGs calculated in TE_1 mode for different CuO_x layer thicknesses (1 nm–10 μm) are shown in Fig. 11. A refractive index of $1.9 + 0.04i$ was used to represent Cu_2O. A Cu-coated PPWG without surface oxide is shown as a control. The propagation losses of the CuO_x/Cu-coated PPWGs with CuO_x thicknesses of <1 μm were equivalent to the losses of Cu-coated PPWGs without oxides, indicating that the CuO_x layer did not influence THz wave propagation. A loss difference was observed when the CuO layer was 5-μm-thick; this was 10% (compared to Cu) at 1 THz. The losses were larger when the layer was 10-μm-thick, thus 31% higher at

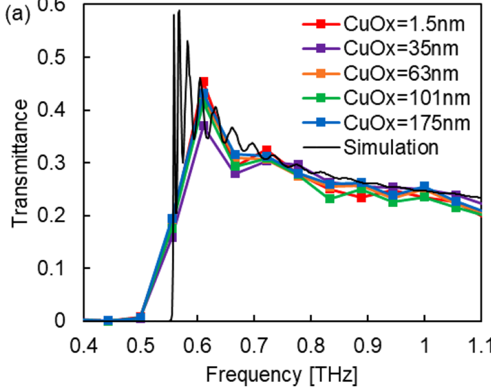

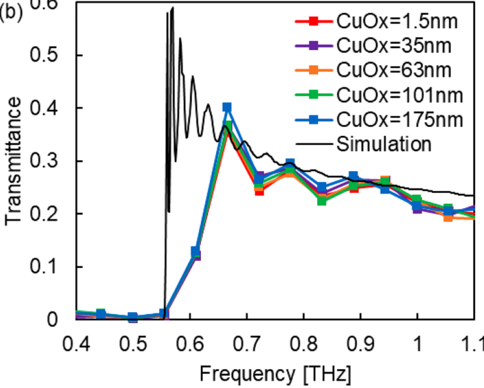

FIG. 9. Transmittance spectra of (a) 2.5-mm- and (b) 5.0-mm-long Cu (300 nm)-coated PPWGs with a thick CuO_x layer on the Cu surface. A corresponding model simulation (black line) for PPWGs composed of PEC is shown for comparison.

Published under an exclusive license by AIP Publishing

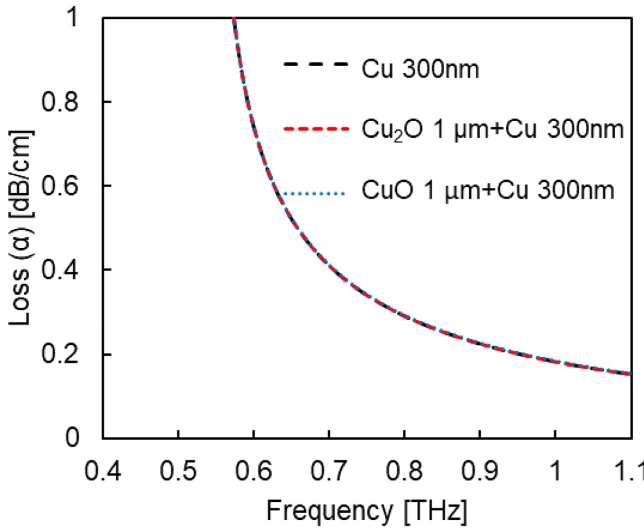

FIG. 10. Propagation losses of PPWGs consisting of 1-μm-thick CuO_x/300-nm-thick Cu/Si in TE_1 mode. The conductivity of the Cu coating was 3.7×10^7 S/m.

0.72 THz and 72% higher at 1.0 THz; however, this was an unrealistic value considering the very slow native oxidation. The same results were obtained for CuO (data not shown).

These investigations were conducted under the assumption of a sufficiently thick Cu film to prevent penetration loss, such that the conductivity of the Cu film remained unchanged. However, if

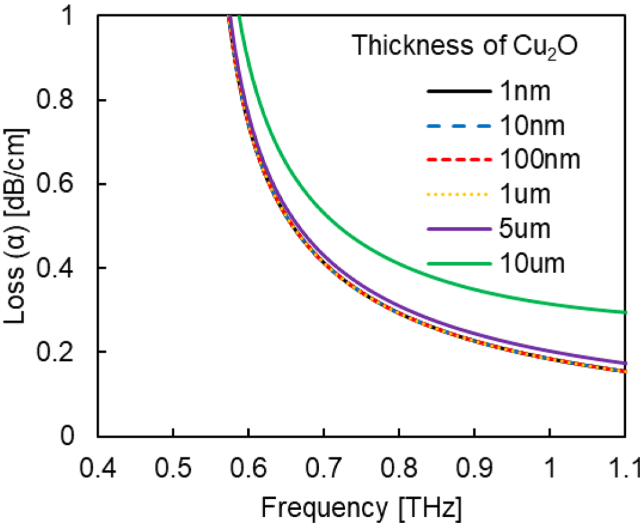

FIG. 11. Propagation losses of Cu_2O/Cu/Si PPWGs in TE_1 mode with different Cu_2O thicknesses, ranging from 1 nm to 10 μm, with an assumed refractive index of 1.9 + 0.04*i*. The thickness of the Cu coating was 300 nm, with a conductivity of 3.7×10^7 S/m.

the Cu film were thinner than the critical film thickness, its conductivity and resulting ohmic loss would continuously increase during the native oxidation. Thus, the thickness of the Cu film should be designed considering the thinning of the Cu film by native oxidation. Some devices are designed to practically adopt a passivation layer (e.g., Au) to prevent the metal coating from experiencing native oxidation (e.g., Cu);[63,64] however, this is unnecessary if the Cu film is sufficiently thick. Thus, the impact of a thin CuO_x layer (<1 μm) on THz wave propagation was found to be negligible, regardless of its thickness. Therefore, we conclude that Cu is a more suitable material than Au for THz application.

VI. REMARKS ON CU DEPOSITION

We identified Cu as the optimal material; an appropriate deposition method for fabrication of metal-coated dielectric THz waveguides is thus required. We previously showed that high-quality films reduced the critical film thickness and also suppressed propagation loss in films thicker than the critical thickness. Consequently, the Cu film must cover the entire surface of a THz waveguide; losses will occur in regions of insufficient thickness. This is not simple; a waveguide has already narrow (submillimeter-scale) features and a high aspect ratio, which makes harder for waveguide integration with other passive devices such as antennas, filters, and resonators for even higher aspect ratio. Therefore, the requirements for deposition are as follows: a high-quality film that is uniformly deposited onto narrow high aspect ratio features. Although electroplating is currently used for THz waveguide fabrication (in part because of the high deposition rate), the propagation loss is not necessarily small. The films may be of poor quality and show low conformality. Although the very thick (500–1000 nm) electroplated Au and Cu films employed in past studies may have been reasonable (given the large critical film thicknesses), a low propagation loss was not expected because the films were of poor quality. High quality and conformality are the primary requirements of Cu deposition, and a deposition rate lower than that of electroplating is acceptable because the critical film thickness is reduced by higher film quality. The leading candidate methods are chemical vapor deposition, atomic layer deposition, and supercritical fluid deposition.[19–23]

VII. CRITICAL FILM THICKNESSES IN OTHER WAVEGUIDE GEOMETRIES

Next, we investigated the generalities of the two key parameters for determining waveguide performance in the THz region—critical film thickness and the propagation loss of a film of thickness greater than the critical thickness—for other geometries, including RWGs and circular waveguides (CWGs). The propagation loss in a film thicker than the critical film thickness was explored as follows. The propagation loss of a metal-coated waveguide with a film thicker than the critical film thickness approximates that of a metallic waveguide. The propagation loss of such a waveguide depends on the geometry. All relevant geometries are general solutions of the Maxwell–Boltzmann equation; they do not involve bouncing waves. Hence, the propagation loss in films thicker than the critical film thickness in other geometries can be estimated without the losses that we obtained experimentally. Only

Published under an exclusive license by AIP Publishing

the bulk conductivity, waveguide size, and frequency are relevant. We now discuss the generality of critical film thickness. As this thickness is determined in the THz region by the ohmic loss alone,[27] it can be calculated from the thickness-dependent conductivity. Note that this is true only in the THz region; the critical film thickness is not determined by thickness-dependent conductivity in the GHz region. In this context, the propagation losses (functions of conductivity and frequency) of metallic RWGs, CWGs, and PPWGs[65] in the THz region should be modified by introducing thickness-dependent conductivities. The propagation losses of such geometries have been described elsewhere.[65] The propagation loss of an RWG in TE_{10} mode can be expressed as follows:

$$\alpha_{\mathrm{RWG(TE_{10})}} = \frac{R_s}{a^3 bk\beta\eta}\left(2b\pi^2 + a^3k^2\right), \tag{7}$$

whereas the propagation loss of a CWG in TE_{11} mode can be expressed as follows:

$$\alpha_{\mathrm{CWG(TE_{11})}} = \frac{R_s}{rk\beta\eta}\left(k_c^2 + \frac{k^2}{2.39}\right), \tag{8}$$

and the propagation loss of a PPWG in TE_1 mode can be expressed as follows:

$$\alpha_{\mathrm{PPWG(TE_1)}} = \frac{2k_c^2 R_s}{k\beta\eta d}. \tag{9}$$

All parameters are explained in Table S1 in the supplementary material; a and b ($a > b$) are the inner dimensions of the rectangular waveguide opening, r is the inner radius of the circular waveguide, δ is the gap distance of the parallel plate, k is the wave number, k_c is the cutoff wave number, β is the propagation constant, and R_s is the surface resistivity of metals; the important factors for determining the two key parameters are k, β, and R_s, where k and β are functions of frequency, while R_s is a function of both frequency and conductivity, which is the only parameter that includes the bulk electrical conductivity ($\sigma_{0,b}$) in Eqs. (7)–(9); it can be expressed as follows:

$$R_s = \sqrt{\frac{\omega\mu_0}{\sigma_{0,b}}}, \tag{10}$$

where μ_0 is the permeability of the bulk metal. Substitution of the thickness-dependent conductivity ($\sigma_{0,f}$) determined by Eq. (4) into $\sigma_{0,b}$ allows us to anticipate the propagation loss depending on film thickness, thus estimating the critical film thickness. From Eqs. (7) to (9), the propagation losses of the RWG, CWG, and PPWG are proportional to R_s, which is inversely proportional to the square root of $\sigma_{0,f}$. Thus, for each of these waveguides, propagation loss is inversely proportional to the square root of $\sigma_{0,f}$; the relative propagation loss depending on film thickness is equivalent, regardless of the geometry. Because the critical film thickness is defined to have a loss 10% larger than the loss of a 500-nm-thick film, it remains constant regardless of geometry. Thus, the critical film thicknesses for the PPWG are equivalent between the RWG and CWG in the THz region.

VIII. CONCLUSIONS

In this study, we investigated suitable metals for coating dielectric THz waveguides, focusing on Au, Cu, Ag, Al, Ni, Cr, and Ti. We evaluated two key parameters for screening metal coatings—critical film thickness and propagation losses for a film with a thickness greater than the critical thickness. We compared experimental observations to calculations obtained using our previously developed physical model. Multi-channel, metal-coated dielectric PPWGs were selected as test structures. The transmittances of 2.5- and 5.0-mm metal-coated PPWGs with different film thicknesses were experimentally measured, and the propagation loss according to thickness was determined. The thickness-dependent conductivities of the metals were experimentally determined, and the propagation losses depending on film thickness were then simulated by the model using the thickness-dependent conductivity results. The good match between the observed and calculated propagation losses of the Au, Cu, Ni, Cr, and Ti demonstrated the generality of the model for different metals. The metals were next compared in terms of the two key parameters estimated by the model, assuming identically high film quality. Ag and Al were also examined. Cu was ultimately recognized as the most suitable metal, i.e., that with the lowest critical film thickness and comparable loss in a film thicker than the critical thickness (with Ag has the smallest value). The critical film thickness depends on film quality (thickness-dependent conductivity in the present case), as does the propagation loss within a film thicker than the critical film thickness. As the differences between the two key parameters were not large among Ag, Au, and Al; they could be used if creating such high-quality films are attainable while creating high-quality Cu films are unreachable. Not only the intrinsic properties of metals but also their deposition methods and conditions affect film quality. Conformality must also be considered; THz waveguides have narrow (submillimeter-scale) features and a high aspect ratio.

Although Cu is considered to be a suitable material, it is prone to native oxidation, which can degrade waveguide performance. Therefore, we experimentally examined the impact of the CuO_x layer on Cu-coated PPWGs. The transmittances of PPWGs with CuO_x layers of various thicknesses (1.5–7.2 nm) created by annealing were measured. We detected no decrease in transmittance, regardless of the presence of a CuO_x layer; thus, native CuO_x, which typically has a thickness of <10 nm even after several years at room temperature, had a negligible impact on transmittance. The impact of a very thick CuO_x layer (35–176 nm) on transmittance was investigated by sputtering CuO_x onto Cu film; the transmittance decrease was also negligible in this experiment. The impact of the CuO_x layer on the propagation loss was further investigated using the extended physical model. The impact of a 1-μm-thick CuO_x layer on propagation loss in Cu-coated PPWGs was found to be negligible, regardless of its oxidation state. The impact of CuO_x layer thickness was further analyzed, and the results showed that the effect of CuO_x was negligible at a thickness of <1 μm, under the assumption that the Cu film underlying the CuO_x layer is not sufficiently thin to alter its conductivity. If the

Published under an exclusive license by AIP Publishing

Cu film is thinner than the critical film thickness, the ohmic loss will increase during the native oxidation. Therefore, the thinning of Cu film by native oxidation should be considered when designing Cu-coated waveguides. Finally, Cu was identified as the most suitable metal for coating dielectric THz wave devices.

We also investigated the generality of the critical film thickness obtained for PPWGs to other waveguide geometries by determining the propagation losses (a function of conductivity and frequency) of metallic RWG and CWG, using thickness-dependent conductivity as input. The critical film thicknesses obtained using PPWGs were equivalent to the thicknesses of RWG and CWG, regardless of waveguide geometry. This method was only feasible for frequencies >0.3 THz, where penetration loss could be neglected. The results confirmed the generality of the critical film thickness for designing metal-coated dielectric THz RWG and CWG devices.

SUPPLEMENTARY MATERIAL

See the supplementary material for details on the cross-sectional images of metal films, transmittances, and propagation losses of fabricated metal-coated PPWG.

ACKNOWLEDGMENTS

This work was supported by Japan Society for the Promotion of Science KAKENHI, JP20H0251.

AUTHOR DECLARATIONS

Conflict of Interest

The authors have no conflicts to disclose.

DATA AVAILABILITY

The data that support the findings of this study are available from the corresponding author upon reasonable request.

REFERENCES

[1]L. Afsah-Hejri, E. Akbari, A. Toudeshki, T. Homayouni, A. Alizadeh, and R. Ehsani, Comput. Electron. Agric. **177**, 105628 (2020).
[2]I. F. Akyildiz, J. M. Jornet, and C. Han, Phys. Commun. **12**, 16 (2014).
[3]W. R. Tribe, D. A. Newnham, P. F. Taday, and M. C. Kemp, "Hidden object detection: Security applications of terahertz technology," Proc. SPIE **5354**, 168 (2004).
[4]L. Yu, L. Hao, T. Meiqiong, H. Jiaoqi, L. Wei, D. Jinying, C. Xueping, F. Weiling, and Z. Yang, RSC Adv. **9**, 9354 (2019).
[5]R. Dickie, R. Cahill, V. Fusco, H. S. Gamble, and N. Mitchell, IEEE Trans. Terahertz Sci. Technol. **1**, 450 (2011).
[6]I. F. Akyildiz, A. Kak, and S. Nie, IEEE Access **8**, 133995 (2020).
[7]F. Sammoura, Y. Cai, C.-Y. Chi, T. Hirano, L. W. Lin, and J.-C. Chia, in *Transducers '05, Digest of Technical Papers* (IEEE, 2005), Vols. 1 and 2, p. 1067.
[8]C. Wang, X. W. Li, Y. X. Huang, W. D. Xu, R. Y. Zhou, R. Q. Wang, L. J. Xie, and Y. B. Ying, Opt. Express **26**, 24992 (2018).
[9]E. G. Geterud, P. Bergmark, and J. Yang, "Lightweight waveguide and antenna components using plating on plastics," in *2013 7th European Conference on Antennas and Propagation (EuCAP), Gothenburg, Sweden* (IEEE, 2013), p. 1812.
[10]C. D. Nordquist, M. C. Wanke, A. M. Rowen, C. L. Arrington, M. Lee, and A. D. Grine, in *2008 IEEE Antennas and Propagation Society International Symposium* (IEEE, 2008), Vols. 1–9, p. 3367.
[11]S. S. Dhillon, M. S. Vitiello, E. H. Linfield, A. G. Davies, M. C. Hoffmann, J. Booske, C. Paoloni, M. Gensch, P. Weightman, G. P. Williams, E. Castro-Camus, D. R. S. Cumming, F. Simoens, I. Escorcia-Carranza, J. Grant, S. Lucyszyn, M. Kuwata-Gonokami, K. Konishi, M. Koch, C. A. Schmuttenmaer, T. L. Cocker, R. Huber, A. G. Markelz, Z. D. Taylor, V. P. Wallace, J. Axel Zeitler, J. Sibik, T. M. Korter, B. Ellison, S. Rea, P. Goldsmith, K. B. Cooper, R. Appleby, D. Pardo, P. G. Huggard, V. Krozer, H. Shams, M. Fice, C. Renaud, A. Seeds, A. Stohr, M. Naftaly, N. Ridler, R. Clarke, J. E. Cunningham, and M. B. Johnston, J. Phys. D: Appl. Phys. **50**, 043001 (2017).
[12]V. Desmaris, D. Meledin, A. Pavolotsky, R. Monje, and V. Belitsky, J. Micromech. Microeng. **18**, 095004 (2008).
[13]C. Jung-Kubiak, T. J. Reck, J. V. Siles, R. Lin, C. Lee, J. Gill, K. Cooper, I. Mehdi, and G. Chattopadhyay, IEEE Trans. Terahertz Sci. Technol. **6**, 690 (2016).
[14]R. Y. Zhu, G. Lipworth, T. Zvolensky, D. R. Smith, and D. L. Marks, IEEE Antennas Wirel. Propag. Lett. **16**, 157 (2017).
[15]O. Glubokov, X. H. Zhao, J. Campion, B. Beuerle, U. Shah, and J. Oberhammer, IEEE Trans. Microw. Theory Tech. **67**, 3696 (2019).
[16]J. Y. Sun and F. J. Hu, Int. J. RF Microw. Comput. Aided Eng. **30**, e21983 (2020).
[17]S. Lucyszyn, F. J. Hu, and W. J. Otter, "Technology demonstrators for low-cost terahertz engineering," in *2013 Asia-Pacific Microwave Conference Proceedings (APMC), Seoul, South Korea* (IEEE, 2013), p. 518.
[18]H. Xin and M. Liang, Proc. IEEE **105**, 737 (2017).
[19]E. T. Eisenbraun, A. Klaver, Z. Patel, G. Nuesca, and A. E. Kaloyeros, J. Vac. Sci. Technol. B **19**, 585 (2001).
[20]A. M. Kia, N. Haufe, S. Esmaeili, C. Mart, M. Utriainen, R. L. Puurunen, and W. Weinreich, Nanomaterials **9**, 1035 (2019).
[21]T. Momose, T. Uejima, H. Yamada, Y. Shimogaki, and M. Sugiyama, Jpn. J. Appl. Phys. **51**, 056502 (2012).
[22]T. Momose, M. Sugiyama, E. Kondoh, and Y. Shimogaki, Appl. Phys. Express **1**, 097002 (2008).
[23]J. M. Blackburn, D. P. Long, A. Cabanas, and J. J. Watkins, Science **294**, 141 (2001).
[24]V. Gerasimov, B. Knyazev, A. Nikitin, and G. Zhizhin, Appl. Phys. Lett. **98**, 171912 (2011).
[25]V. V. Gerasimov, B. A. Knyazev, A. G. Lemzyakov, A. K. Nikitin, and G. N. Zhizhin, J. Opt. Soc. Am. B **33**, 2196 (2016).
[26]S. Atakaramians, S. Afshar V, T. M. Monro, and D. Abbott, Adv. Opt. Photonics **5**, 169 (2013).
[27]Y. Huang, K. Konishi, M. Deura, Y. Shimoyama, J. Yumoto, M. Kuwata-Gonokami, Y. Shimogaki, and T. Momose, J. Appl. Phys. **130**, 055104 (2021).
[28]S. Pandey, B. Gupta, and A. Nahata, Opt. Express **21**, 24422 (2013).
[29]J. Hu, S. Y. Xie, and Y. Zhang, IEEE Microw. Wirel. Compon. Lett. **22**, 636 (2012).
[30]W. R. McGrath, C. Walker, M. Yap, and Y.-C. Tai, IEEE Microw. Guided Wave Lett. **3**, 61 (1993).
[31]B. Bowden, J. A. Harrington, and O. Mitrofanov, Opt. Lett. **32**, 2945 (2007).
[32]J. A. Harrington, P. Pedersen, B. Bowden, A. Gmitter, and E. Mueller, "Hollow Cu-coated plastic waveguides for the delivery of THz radiation," Proc. SPIE **5727**, 143 (2005).
[33]M. Miyagi, A. Hongo, Y. Aizawa, and S. Kawakami, Appl. Phys. Lett. **43**, 430 (1983).
[34]Y. Arita, N. Awaya, K. Ohno, and M. Sato, "CVD copper metallurgy for ULSI interconnections," in *International Electron Devices Meeting (IEDM)* (IEEE, 1990), p. 39.
[35]B. Zhao, T. Momose, and Y. Shimogaki, Jpn. J. Appl. Phys. **45**, L1296 (2006).
[36]J. S. Huo, R. Solanki, and J. McAndrew, J. Mater. Res. **17**, 2394 (2002).
[37]M. Razanoelina, S. Ohashi, I. Kawayama, H. Murakami, A. F. Dégardin, A. J. Kreisler, and M. Tonouchi, Opt. Lett. **42**, 3056 (2017).
[38]R. Mendis and D. M. Mittleman, J. Opt. Soc. Am. B **26**, A6 (2009).
[39]N. Laman and D. Grischkowsky, Appl. Phys. Lett. **90**, 122115 (2007).

Published under an exclusive license by AIP Publishing

[40]N. Laman and D. Grischkowsky, Appl. Phys. Lett. **93**, 051105 (2008).
[41]J. W. Lim, K. Mimura, and M. Isshiki, Appl. Surf. Sci. **217**, 95 (2003).
[42]K. Mech, R. Kowalik, and P. Zabinski, Arch. Metall. Mater. **56**, 122115 (2011).
[43]F. Sanjuan and J. O. Tocho, "Optical properties of silicon, sapphire, silica and glass in the terahertz range," in *Latin America Optics and Photonics Conference, OSA Technical Digest (online)* (Optica Publishing Group, 2012), p. LT4C. 1.
[44]F. Smits, Bell Syst. Tech. J. **37**, 711 (1958).
[45]G. Gallot, S. P. Jamison, R. W. McGowan, and D. Grischkowsky, J. Opt. Soc. Am. B **17**, 851 (2000).
[46]S. P. Jamison, R. W. McGowan, and D. Grischkowsky, Appl. Phys. Lett. **76**, 1987 (2000).
[47]R. Mendis and D. M. Mittleman, Opt. Express **17**, 14839 (2009).
[48]A. Bandyopadhyay, A. Sengupta, V. Johnson, J. A. Harrington, and J. F. Federici, "Characterization of hollow polycarbonate metal waveguides using terahertz time domain spectroscopy," Proc. SPIE **6120**, 61200B (2006).
[49]S. Lucyszyn, PIERS Online 4, 686 (2008).
[50]W. M. Haynes, *CRC Handbook of Chemistry and Physics* (CRC Press, 2014).
[51]D. Gall, J. Appl. Phys. **127**, 050901 (2020).
[52]D. Gall, J. Appl. Phys. **119**, 085101 (2016).
[53]S. L. Udachan, N. H. Ayachit, and L. A. Udachan, Ingeniería Universidad **23**, 1 (2019).
[54]B. Singh and N. Surplice, Thin Solid Films **10**, 243 (1972).
[55]F. Benson and D. H. Steven, *Rectangular-Waveguide Attenuation at Millimetre Wavelengths* (IET, 1963), p. 1008.
[56]S. Saito and K. Kurokawa, Proc. IRE **44**, 35 (1956).
[57]A. H. White and L. H. Germer, Trans. Electrochem. Soc. **81**, 305 (1942).
[58]T. N. Rhodin, J. Am. Chem. Soc. **72**, 5102 (1950).
[59]J. J. D. Leon, D. M. Fryauf, R. D. Cormia, and N. P. Kobayashi, "*Study of the formation of native oxide on copper at room temperature*," Proc. SPIE **9924**, 99240O (2016).
[60]K. Singh, S. CK, A. Bandyopadhyay, and A. Sengupta, "Characterization of hollow-core-metal waveguide using broadband THz time domain spectroscopy for high-pressure and temperature sensor," Proc. SPIE **11685**, 1168514 (2021).
[61]Y. P. Yang, W. Z. Wang, Z. W. Zhang, L. L. Zhang, and C. L. Zhang, J. Phys. Chem. C **115**, 10333 (2011).
[62]S. P. P. Jones, S. M. Gaw, K. I. Doig, D. Prabhakaran, E. M. H. Wheeler, A. T. Boothroyd, and J. Lloyd-Hughes, Nat. Commun. **5**, 3787 (2014).
[63]X. B. Shang, P. Penchev, C. Guo, M. J. Lancaster, S. Dimov, Y. L. Dong, M. Favre, M. Billod, and E. de Rijk, IEEE Trans. Microw. Theory Tech. **64**, 2572 (2016).
[64]A. von Bieren, E. de Rijk, J. P. Ansermet, and A. Macor, "Monolithic metal-coated plastic components for mm-wave applications," in *2014 39th International Conference on Infrared, Millimeter, and Terahertz Waves (IRMMW-THz), Tucson, AZ* (IEEE, 2014).
[65]D. M. Pozar, *Microwave Engineering* (John Wiley & Sons, 2011).

Published under an exclusive license by AIP Publishing